Magnetic properties of FeCo nanoclusters on Cu(100): *Ab initio* calculations

C. Etz,[1] B. Lazarovits,[2] J. Zabloudil,[1] R. Hammerling,[1,3] B. Újfalussy,[2] L. Szunyogh,[4] G. M. Stocks,[5] and P. Weinberger[1]

[1]*Center for Computational Materials Science, Technical University Vienna, A-1060, Gumpendorferstrasse 1a, Vienna, Austria*
[2]*Research Institute for Solid State Physics and Optics of the Hungarian Academy of Sciences, Konkoly-Thege M. út 29-33., H-1121 Budapest, Hungary*
[3]*Wolfgang Pauli Institute c/o Fak. f. Mathematik, University of Vienna, A-1090, Nordbergstrasse 15, Vienna, Austria*
[4]*Department of Theoretical Physics, Budapest University of Technology and Economics, Budafoki út 8., H-1521 Budapest, Hungary*
[5]*Materials Science and Technology Division, Oak Ridge National Laboratory, Oak Ridge, Tennessee 37831, USA*

We present *ab initio* calculations of the magnetic moments and magnetic anisotropy energies of small FeCo clusters of varying composition on top of a Cu(100) substrate. Three different cluster layouts have been considered, namely, 2×2, 3×3, and crosslike pentamer clusters. The ratio of Co atoms with respect to the total number in a chosen cluster ("concentration") was varied and all possible arrangements of the atomic species were taken into account. Calculations have been performed fully relativistic using the embedded-cluster technique in conjunction with the screened Korringa-Kohn-Rostoker method and the magnetocrystalline anisotropy energy (MAE) has been evaluated by means of the magnetic force theorem. A central result of the investigations is that the size of the magnetic moments of the individual Fe and Co atoms and their contributions to the anisotropy energy depend on the position they occupy in a particular cluster and on the type and the number of nearest neighbors. The MAE for the 2×2 and 3×3 clusters varies with respect to the concentration of Co atoms in the same manner as the corresponding monolayer case, whereas the pentamer clusters show a slightly different behavior. Furthermore, for the clusters with an easy axis along a direction in the surface plane, the MAE shows a significant angular dependence.

I. INTRODUCTION

Surface-supported nanoparticles of magnetic atoms are generating much interest nowadays, because of potential applications in nonvolatile magnetic storage media. In the last few years, magnetic nanostructures were investigated experimentally in terms of various different methods, such as scanning tunneling microscopy (STM), x ray magnetic cluster dichroism (XMCD), and magneto optical kerr effect (MOKE).[1–6] In using these techniques together with phenomenological models[7] and sum rules[8] it was possible to infer the high anisotropies and orbital moments of single magnetic adatoms on a nonmagnetic substrate. Eventually it is the ambition of experimental methods to produce and manipulate nanostructures on an atom-by-atom level which is currently attempted by means of, for example, magnetic tunnel tips.[9] Furthermore, by combining magnetic and nonmagnetic materials such as CoPt,[1] or two different magnetic species such as FeCo (Ref. [10]) to form nanoclusters, interesting structural arrangements and enhanced, tunable magnetic properties are obtained.

A key challenge for experimental methods is, in view of the fabrication of so-called bit-patterned media,[11,12] to produce grains of controlled size and position, of known composition, and with sharply defined magnetic properties.[13,14] This would pave the way to increase achievable areal densities[15] of magnetic recording media by several orders of magnitude.[13,16–19]

One of the main issues is the magnetic anisotropy energy which determines the orientation of the magnetization of a cluster with respect to the surface. Large magnetocrystalline anisotropy energy (MAE) barriers can stabilize the magneti-zation direction in the cluster and a stable magnetic bit can be created.[20,21] In contrast to bulk solids, clusters deposited on surfaces offer additional degrees of freedom to change the MAE. It can be influenced by the shape, size, and composition of the cluster and by the substrate. In this paper we will concentrate on the investigation of the effects of composition and of the details of the atomic arrangements within magnetic clusters on the anisotropy by means of *ab initio* calculations.

The information learned from these computational studies can be used later to construct nanostructures with optimized properties. Moreover, these studies can be compared to calculations made for monolayers using the coherent-potential approximation (CPA) and relate the impact of the local environment to the mean-field solution.

II. THEORETICAL APPROACH AND COMPUTATIONAL DETAILS

Self-consistent, relativistic calculations for FeCo clusters on a Cu(100) surface have been performed using the embedded-cluster technique[22] within multiple-scattering theory (MST) which enables the treatment of a finite cluster of impurities embedded into a two-dimensional translational invariant semi-infinite host. Within MST the electronic structure of a cluster of embedded atoms is described by the so-called scattering path operator (SPO) matrix given by the following Dyson equation:[22]

$$\tau_C(\epsilon) = \tau_h(\epsilon)\{1 - [t_h^{-1}(\epsilon) - t_C^{-1}(\epsilon)]\tau_h(\epsilon)\}^{-1}, \quad (1)$$

where $\tau_C(\epsilon)$ comprises the SPO for all sites of a given finite cluster C embedded in a host system, $t_h(\epsilon)$ and $\tau_h(\epsilon)$ denote
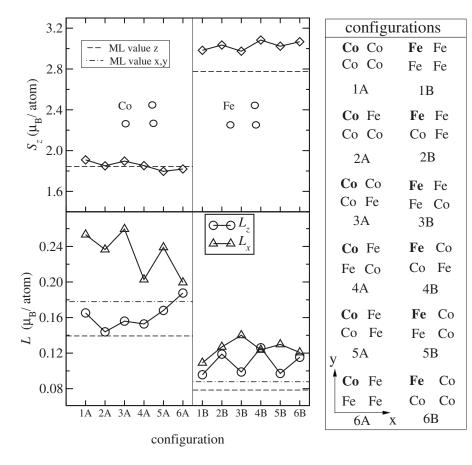
FIG. 1. Spin and orbital magnetic moments of selected Co (left panel) and Fe (right panel) atoms as a function of all cluster configurations possible (Co: iA, Fe: iB, $i=1,\ldots,5$), see the scheme to the right. The dashed horizontal lines refer to the corresponding Fe/Cu(100) or Co/Cu(100) monolayer values for a magnetization along the coordinate z axis. The dash-dotted horizontal lines refer to those with the magnetization along the $x(y)$ axis. The investigated atom is indicated by boldface letters.

the single-site scattering matrix and the SPO of the unperturbed host sites in cluster C, respectively, while $t_C(\epsilon)$ stands for the single-site scattering matrix of the impurity atoms. Once $\tau_C(\epsilon)$ is known all corresponding local quantities, i.e., charge and magnetization densities, spin and orbital moments, as well as the total energy can be calculated. In all cases the atomic sphere approximation (ASA) was applied.

Self-consistency is achieved by varying the effective potentials and exchange fields using the local-density functionals of Ceperley-Alder (in the parametrization due to Perdew and Zunger)[23] and solving the Poisson equation as described in Ref. 22. In all self-consistent calculations for the embedded clusters the orientation of the magnetization was chosen to point uniformly along the surface normal (z axis). For the calculation of the t matrices and for the multipole expansion of the charge densities (needed to evaluate the Madelung potentials), a cutoff for the angular momentum expansion of $l_{max}=2$ was used.

The host and the cluster sites refer to the positions of an ideal fcc lattice with the experimental lattice constant of Cu ($a=3.6147$ Å). Structural relaxations of both the cluster-substrate distance as well as of the bond length between cluster atoms, which may also affect the magnetic properties,[24–27] have been neglected. As the atomic radii of the elemental Fe, Co, and Cu are similar, relaxations can be expected to be relatively small. For the semi-infinite Cu(100) host a self-consistent fully relativistic calculation was performed in terms of the screened Korringa-Kohn-Rostoker method[28] using 66 $k_{\parallel}$ points for the irreducible Brillouin-zone integration and 16 energy points for the energy integrations

along a semicircular contour in the complex energy plane by means of a Gaussian quadrature.

The MAE is defined as the difference in the total energies of the clusters with the magnetization along two different directions. While in the bulk or thin films of ferromagnetic materials the preferred magnetization direction will be along one of the principle crystal axes, this will not be the case in composite nanoclusters. Depending on the shape and the composition of the clusters the easy (or hard) axis can be found along a (arbitrary) direction α $=(\sin\theta\cos\varphi,\sin\theta\sin\varphi,\cos\theta)$. In terms of the magnetic force theorem,[29] the MAE is given by the energy difference between the band energies corresponding to two orientations, α and β, of the magnetization

$$\Delta E_{\alpha\beta} = E_{\alpha}^{b} - E_{\beta}^{b}, \qquad (2)$$

which were evaluated using the self-consistent potentials taken from the calculation where the orientation of the magnetization was chosen to be perpendicular to the surface (z axis). Here the band energy is actually the grand canonical potential, which at $T=0$ K is given by

$$E_{\alpha}^{b} = \int_{\varepsilon_B}^{\varepsilon_F} (\varepsilon - \varepsilon_F) n(\varepsilon, \alpha) d\varepsilon, \qquad (3)$$

where ε_B is the bottom of the valence band and $n(\varepsilon, \alpha)$ denotes the density of states for the magnetization pointing uniformly along direction α. Use of the force theorem in the present context seems justified as the atomic species considered are 3d transition metals for which the approximations
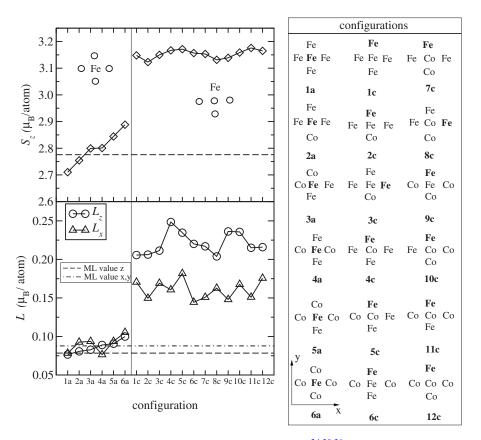
FIG. 2. Spin and orbital magnetic moments of a selected Fe atom as a function of its position in the cluster and of the number of Co neighbors. For the actual configuration see the panel to the right. The dashed horizontal lines refer to the corresponding Fe/Cu(100) monolayer values with the magnetization along the coordinate z axis. The dash-dotted horizontal lines refer to those with the magnetization along the $x(y)$ axis.

due to the first-order perturbation theory are legitimate.[24,30,31]

For the present calculations only the nearest-neighbor shell of host and vacuum sites surrounding the Fe and Co atoms forming the clusters was taken into account. Our previous convergence studies[22] of the magnetic properties of pure Fe clusters as a function of the number of shells demonstrated that for a Ag substrate considering only the first shell suffices. For a Cu host, being a noble metal with similar properties as Ag, a first shell of neighbors can therefore safely be assumed to be adequate. In the following, the term "cluster" will be used (for simplicity) to denote the set of Co and/or Fe atoms only.

The dimensions of the clusters were varied in the following way: we chose a 2×2, a crosslike pentamer, and a 3×3 cluster as illustrated, e.g., in Ref. 22. The atoms in the clusters occupy nearest-neighbor positions of the ideal fcc (100) geometry. Taking the first shell, the studied systems actually consist of 30 ASA spheres in the 2×2 case, 40 for the pentamer cluster, and 53 in the case of the 3×3 cluster. These systems refer to the first three layers of a parent fcc lattice. The first layer is formed by atoms of the substrate, the second layer contains Co and/or Fe atoms and surrounding vacuum spheres, and the third layer is formed only by vacuum spheres. We varied the "concentration" of the Co atoms, namely, the ratio of Co atoms with respect to the total number of Co and Fe atoms in the clusters and considered, in addition, for each concentration also all possible configurations, i.e., arrangements of the atoms in the cluster.

In the following sections, the most important magnetic properties of the clusters (detailed for each constituent atom) are discussed, namely, the magnetic spin and orbital moments and the anisotropy energy. All quantities have been studied with respect to the clusters' size, to the constituent atoms' concentrations, and to the different positions of the atoms within the clusters. Furthermore, the results are compared to those of a monolayer of either Co or Fe, in particular cases also to a monolayer of Co_xFe_{1-x} on top of Cu(100).

III. RESULTS AND DISCUSSION

A. Magnetic moments

One of the central results of all previous studies of (pure) nanoclusters has been that the spin-only magnetic moments show a negligible dependence on the direction of the magnetization, while the orbital moments depend significantly on it.[22,31,35,36] However, it will be shown that in clusters of composite materials, there appears to be a significant correlation between the size of the spin and the orbital magnetic moments and the specific positions of the atoms. As far as the spin moments are concerned, it will be pointed out that for some clusters this dependency is also connected with the atomic coordination, and hence it is due to the position occupied by the atom. In order to present the large amount of data in a compact way, below, the results for the magnetic moments are summarized separately for each type of cluster that has been studied.

1. 2×2 cluster

We start our discussion with the magnetic moments for the smallest cluster studied, namely, for the tetramer. In Fig. 1, the variation of the spin (S) and orbital moments (L) of a selected Co and an Fe atom is plotted for different cluster configurations (full lines), together with the corresponding
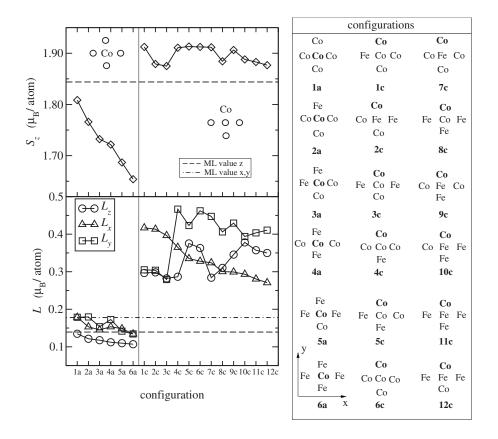
FIG. 3. Spin and orbital magnetic moments of a selected Co atom as a function of the position occupied in the cluster and of the number of Fe neighbors. For the actual configuration, see the panel to the right. The dashed horizontal lines refer to the corresponding Co/Cu(100) monolayer values along the coordinate z axis. The dash-dotted horizontal lines refer to those with the magnetization along the $x(y)$ axis.

Fe or Co monolayer values (dashed and dash-dotted lines). The spin magnetic moment of the chosen Co atom, even in a small four atom cluster, has almost the same value as in the Co monolayer case, whereas the Fe magnetic moments in the cluster are enhanced with respect to the Fe monolayer due to the reduced coordination number. In the 2×2 cluster, all the positions are geometrically equivalent; however, the orbital magnetic moments are still sensitive to the type of the atoms occupying the different positions in the cluster, or, shortly to the local environment (see configurations 4A and 5A, and 4B and 5B). As can be noticed from the left panel of Fig. 1 the orbital moment values of the investigated atoms are more sensitive to the environment than those of the spin moment. The value of the orbital moment on an Fe or Co atom can vary by more than 30% depending on its surrounding atoms. While the spin moments have a very small variation with respect to the changes in the direction of the magnetization (from in plane to out of plane), for the orbital moments the difference can be significant. For the Co atoms the values of L_x are higher than those for L_z so it has to be expected that the Co atoms have a preferred in-plane direction for the magnetization. The value with respect to L_z of the Co atom has a minimum when it has one Fe nearest neighbor (NN) and increases with the number of Fe atoms in the cluster. Contrary, the same quantity of an Fe atom shows only minor oscillations when the number of the Co NN changes.

2. Pentamer cluster

The distinctive feature of a pentamer cluster—in comparison with a quadratic 2×2 cluster—is the existence of two geometrically nonequivalent positions. While the atom at the

central position in the cluster has four coordinated atoms, an atom at a corner position has only one. Figure 2 illustrates the variation of S and L of particular Fe atoms with respect to changes of neighboring atoms. In the left panel the magnetic moments of the central Fe atom are displayed and in the right panel those of an Fe atom in a corner position are shown.

Although the value of the spin and the orbital moments of the central Fe atoms increase monotonously with the number of Co NNs, they are still in a range of approximately $\pm0.1\mu_B$ with respect to the monolayer value of $2.85\ \mu_B$ of Fe/Cu(100). The spin moment shows linear dependence on the number of the Co NNs. In contrast, the values of the corner atoms, while being much higher than in the monolayer case, exhibit a less pronounced dependence on the environment. Taking a closer look at the orbital moments, we see that they are significantly larger than in the monolayer $(0.078\mu_B)$ only for corner atoms for which the value ranges between 0.2 and $0.23\mu_B$, while for the central atoms they vary smoothly and are close to the monolayer value. The difference in the orbital moment values, namely, between L_z and L_x, is about $0.06\mu_B$ and suggests that the corner Fe atoms prefer an out-of-plane direction for the magnetization. Finally, the spin moments of an Fe atom at a corner position is increased dramatically by approximately $0.4\mu_B$ as compared to the value in an Fe monolayer on Cu(100) $(2.77\mu_B)$.

Figure 3 shows the same quantities and additionally the orbital moment for the magnetization pointing along the y axis, L_y, now for a Co atom in the central and at a corner position. Contrary to the case of Fe, the spin moment of a central Co atom is smaller than the corresponding monolayer value $(1.84\mu_B)$ in every configuration. Similarly to the Fe case the dependence of S of the central Co atom on the
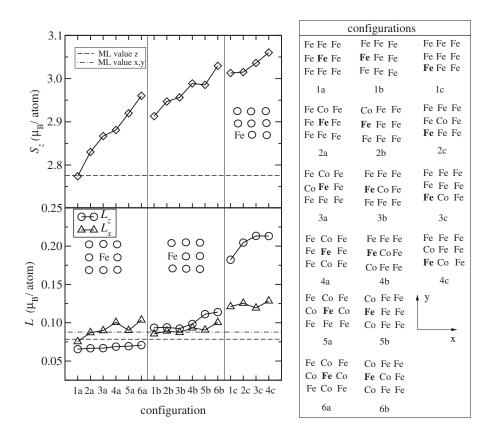
FIG. 4. Spin and orbital magnetic moments of a selected Fe atom in a 3×3 cluster as a function of its position and the number of Co NN for selected cluster configurations (see the panel to the right). The dashed horizontal lines refer to the corresponding Fe/Cu(100) monolayer values with the magnetization along the coordinate z axis. The dash-dotted horizontal lines refer to those with the magnetization along the $x(y)$ axis.

number of Fe NNs is linear but with opposite sign. The decreased spin moment attains its smallest value when the Co atom is surrounded by Fe atoms only (configuration 6a in Fig. 3). Then again, the magnetic moment of a Co atom positioned at a corner is larger than in the monolayer. This is not primarily due to the enhancement of the spin moment but to that of the orbital moment. In the lower panel of Fig. 3 the orbital moments are plotted for magnetizations along the z direction and along the in-plane x and y directions. It can be seen that a central Co atom shows only a small anisotropy of L and a slight dependence on the cluster configuration. At a corner position, a Co atom exhibits a much more pronounced anisotropy and for configurations 1c-3c L_x is largest, assuming a given orientation of the clusters with respect to in-plane x-y coordinate system as illustrated in the legend of Fig. 3. For all other configurations the orbital moment along the y direction becomes largest and is significantly enhanced in comparison to the monolayer case. The reason for the strong increase of the orbital moment of the Fe and Co atoms at corner positions has been discussed[22] for pure Fe, Co, and Ni clusters and can be traced back to the anisotropic environment and reduced coordination number. In the present study this effect is combined with the changes of the magnetic properties due to the different chemical order of the two constituents forming the cluster.

3. 3×3 cluster

The magnetic moments for the three geometrically inequivalent positions (center, edge, and corner) of Fe atoms are displayed in Fig. 4 for selected cluster configurations. Starting in each case from a pure Fe cluster, the NN positions

are successively substituted with Co atoms until all NN sites are occupied exclusively by Co atoms. The only exception is configuration 2c where a second NN has been considered.

As a first observation it can be seen that the spin moments in the pure clusters depend on the position of the Fe atom. The values differ by approximately $0.1\mu_B$ when comparing them at center and center of edge positions. At a corner position the spin moment is further enhanced by $0.1\mu_B$ compared to the edge position. In addition there appears to be an almost linear dependence on the number of coordinated Co atoms at NN sites. While it is interesting to observe that the spin moment of a central Fe atom in a pure Fe cluster is practically identical to the monolayer value, the largest moment of $3.06\mu_B$ is found when an Fe corner atom is coordinated by two Co atoms.

The orbital moments of a central Fe atom are almost identical to their values in a monolayer, with L_x being slightly larger than L_z, exhibiting negligible dependence on the local environment. Similarly, at an edge the orbital moments do not differ significantly from the monolayer values, and are practically independent of the number and position of Co NN. However, L_z is now augmented in comparison to L_x. Most notably the Fe atom located at a corner shows a much more significant enhancement of L_z and is further increased as more Co NNs are added. This can be directly related to the anisotropic surrounding at that position and reduced coordination number, as was already seen in the case of smaller clusters. L_y of Fe atoms does not differ significantly from L_x and therefore has not been included in Figs. 1, 2, and 4.

Independent of the position assumed by the Co atom in the cluster, the spin moments decrease almost monotonously with increasing number of Fe NN (see Fig. 5). Except for
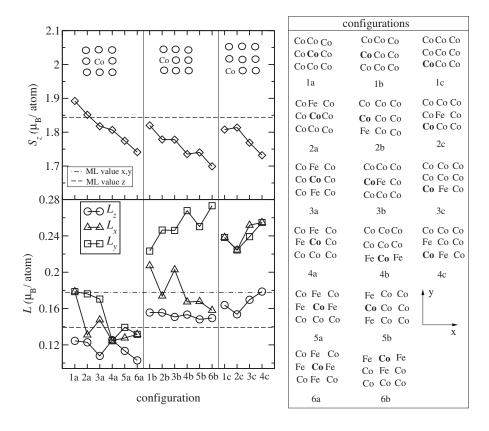
FIG. 5. Spin and orbital magnetic moments of a selected Co atom in a 3×3 cluster as a function of its position and the number of Fe NN for selected cluster configurations (see the panel to the right). The dashed horizontal lines refer to the corresponding Co/Cu(100) monolayer values with the magnetization along the coordinate z axis. The dash-dotted horizontal lines refer to those with the magnetization along the $x(y)$ axis.

configurations 1a and 2a, all values are smaller than the monolayer ones.

Again the orbital moments show a dependence on the position that the Co atom occupies in the cluster. However, L_x, L_y, and L_z depend in different ways on the addition of Fe atoms on the NN sites. While at an edge position L_z is practically unchanged, L_x shows an oscillatory behavior and L_y experiences a strong enhancement as illustrated in the lower panel of Fig. 5. Then again, a Co atom at a corner has a larger L_x almost identical to L_y, and the difference to L_z is approximately constant.

In order to summarize the data discussed above, in Fig. 6 the variation of the spin and orbital magnetic moments averaged over all the configurations for a given Co concentration has been plotted. One can see that the difference in the averaged values of the 3×3 and 2×2 clusters is very small for both S_z and L_z. The atoms within a pentamer cluster exhibit a larger orbital moment with respect to the value of a monolayer of Co_xFe_{1-x} on Cu(100), and also compared to the values in the 2×2 and 3×3 cases. The variation of the spin moments with respect to the Co concentration is linear, just as in the monolayer case, whereas the orbital moment has a more complex behavior. This can be related to the reduced symmetry of the local environment and to the higher ratio of corner atoms in these clusters.

B. Magnetic anisotropy energy

In principle, there are two basic contributions to the magnetic anisotropy energy. One contribution is the so-called shape anisotropy (also referred to as demagnetization or dipole-dipole energy) which is, however, quite small (in the

μeV range) if the clusters are small and of square shape. Due to the strong anisotropy of the orbital moments, and the dependence of both, the spin and the orbital moments on the local environment, this energy is nevertheless enhanced in comparison to pure clusters. However, in this case it is negligible compared to the other contribution to the magnetic anisotropy, namely, the magnetocrystalline anisotropy energy which is caused by spin-orbit coupling of the electrons in a magnetic material. This energy is rather sensitive to the local environment and due to the arrangement of atoms, a magnetization along certain orientations is energetically preferred. Subsequently it will be shown that the magnetocrystalline anisotropy is closely related to the structure and symmetry of the investigated clusters.

The MAE of the three cluster types has been investigated with respect to perpendicular orientations of the magnetization along the coordinate axes, as well as according to the dependence on the azimuth angle φ. To proceed systematically, our discussion will start with the magnetization along x, y, and z, and will then focus on the angular dependence of the MAE.

We compare the results for the 3×3 clusters with those for one monolayer, in Fig. 7, where the configuration-averaged MAE with respect to in-plane (along the x axis) and out-of-plane (along the z axis) magnetization, $\langle\Delta E\rangle_\perp =\langle E_x^b-E_z^b\rangle$, is displayed as a function of the Co concentration. The size of the anisotropy energy is strongly influenced by specific cluster configurations. In some cases the type of the configuration may even be responsible for a change in the preferred orientation of the easy axis as is the case of $x=0.44\%$ Co and $x=0.55\%$ Co. Starting from a pure Fe cluster, which has a large anisotropy energy (+0.6 meV/at.), fa-
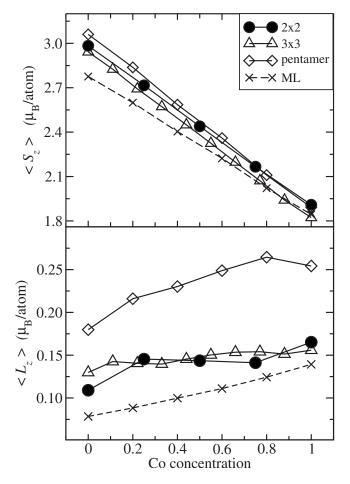
FIG. 6. Spin and orbital moments averaged over all the configurations for a given Co concentration. ($\bullet$: 2×2 cluster; $\diamond$: pentamer cluster; $\triangle$: 3×3 cluster) The dashed line refers to the case of a $Co_x Fe_{1-x}$ monolayer on Cu(100).
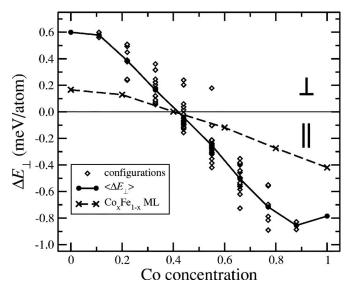

FIG. 7. Magnetic anisotropy energy as a function of the Co concentration: distribution of the anisotropy energies for 3×3 clusters as a function of the clusters configuration (diamonds); the anisotropy energy $\langle \Delta E_\perp \rangle = \langle (\Delta E_{xz} + \Delta E_{yz})/2 \rangle$, where $\langle \rangle$ refers to the average over all configurations (solid line); anisotropy energy for $Co_x Fe_{1-x}/Cu(100)$ monolayer (dashed line). The index $\perp$ indicates that the MAE is calculated as the energy difference between the (surface) normal z and the in-plane x or y direction.

voring out-of-plane orientation, the increase in the Co concentration is responsible for a decreasing anisotropy energy until the easy axis prefers an in-plane orientation. Then a further increase in the Co concentration leads to an augmentation of the in-plane anisotropy. The general trend, however, is very similar to the one obtained in a CPA calculation for a monolayer of $Co_x Fe_{1-x}/Cu(100)$. In comparison to the MAE calculated for a monolayer of $Co_x Fe_{(1-x)}/Cu(100)$ (dashed line) the values for the 3×3 clusters are about three times larger.

It has been suggested by Bruno[7] and Gambardella *et al.*[4,32] that the anisotropy energy is strongly related to the anisotropy of the orbital moments. We investigated the orientation of the MAE with respect to the variation of the orbital moments for the 3×3 clusters, by choosing a configuration with high planar symmetry and applying it to two different concentrations ($Fe_4 Co_5$ and $Fe_5 Co_4$). In order to investigate the correspondence between the orbital moment anisotropy and the MAE, in Fig. 8, the values of the MAE and of the orbital moment per atom are plotted with respect to the positions occupied in the cluster. For the two selected clusters, three different magnetization directions ($\mathbf{M} \| z$, $\mathbf{M} \| x$, and $\mathbf{M} \| y$) were considered. The rule is strictly followed in

the case of $Fe_4 Co_5$ and stands for almost all atoms in $Fe_5 Co_4$, except for the central Fe (i.e., Fe_4) which actually has a very small orbital moment anisotropy (Fig. 8, upper panel). The equivalent positions within a 3×3 cluster (labeled by the same number) are schematically represented in the upper part of Fig. 8. For the sake of simplicity, in this figure only the values for nonequivalent positions are presented. The nonequivalence between positions 2 and 3 is only due to the planar symmetry, which can also be seen from the interchange of the values for L_x and L_y. While the Fe atoms give an out-of-plane contribution to the MAE, the Co atoms have a tendency to an in-plane magnetization. The values of the atomic contributions (from both Fe and Co) vary with the position of the atom within the cluster and increase with increasing coordination number. Figure 8 emphasizes the high sensitivity of the contribution to the MAE of individual atoms on their positions in the cluster. While rather large anisotropy energies can be associated with a particular atom (e.g., 1.2 meV for an Fe atom at a corner in the $Fe_4 Co_5$ cluster) the 3×3 cluster in the left panel of Fig. 8 has an MAE of only about 0.15 meV/at. This example illustrates that the preferred magnetization direction of the cluster as a whole results from an interplay of contending tendencies of the cluster constituents. That different components contribute with different signs to the MAE has been previously observed, e.g., in Co/Pd interfaces.[33]

It is interesting to compare also the configuration-averaged MAE, which is thought to be measured in experimental situations of the 2×2 and 3×3 with those of the pentamer clusters as in Fig. 9. One notices that the MAE of the 2×2 and 3×3 clusters have the same tendency as in the monolayer case, whereas for the pentamer clusters the situa-
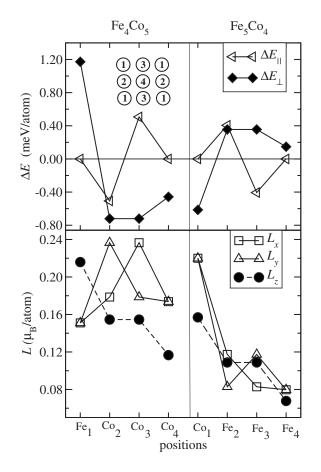
FIG. 8. MAE contributions (upper panel) and orbital magnetic-moment variation (lower panel) per atom for Fe_4Co_5 and Fe_5Co_4. The full circles, squares, and triangles refer in turn to L_z, L_x, and L_y. In the case of Fe_4Co_5, the Fe is in position 1 (denoted by Fe_1) and Co are in positions 2, 3, and 4 (denoted in turn by Co_2, Co_3, and Co_4); in the case of Fe_5Co_4, the Co is in position 1 and the Fe are in positions 2, 3, and 4. (L^{Co} in Co/Cu(100) is $0.139\mu_B$/at.; L^{Fe} in Fe/Cu(100) is $0.08\mu_B$/at.). The triangles and full diamonds refer to $\Delta E_\parallel$ and $\Delta E_\perp$, respectively. $\Delta E_\parallel = \Delta E_{yx}$ and $\Delta E_\perp = (\Delta E_{xz}+\Delta E_{yz})/2$. The indices $\perp$ and $\parallel$ indicate that the MAE is calculated once for the magnetization switch from the normal z towards the in-plane x (y, respectively) direction and then for the in-plane anisotropy between the x and y directions.

tion is different. The larger values for most concentrations in that case are due to the high ratio of corner atoms which have a reduced coordination and whose contributions to the MAE are consequently the largest. In all the cases we have a change of direction of the easy axis with respect to the concentration. For the 2×2 and 3×3 clusters this change occurs at approximately the same concentration ($\sim$40% Co), while for the pentamer cluster, the Co concentration at which the MAE direction changes is higher ($\sim$70%). In the lower panel of Fig. 9 we show that the behavior of the MAE follows closely the averaged orbital moment anisotropy.

The previous sections have focused on the energy difference between the directions along the coordinate axes x, y, and z only. However, one can expect uniaxial anisotropies of the in-plane magnetization along intermediate directions due to the symmetry of a specific cluster configuration. Hence in
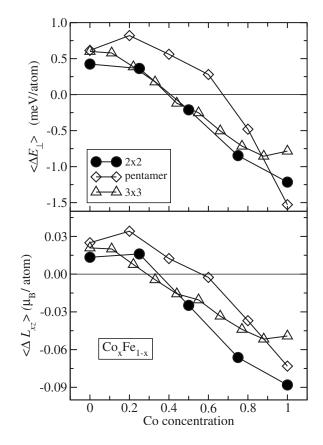

FIG. 9. Upper panel: MAE per atom for the 2×2, 3×3, and the pentamer cluster, averaged over all configurations with respect to the Co concentration. $\langle\Delta E_\perp\rangle=\langle(\Delta E_{xz}+\Delta E_{yz})/2\rangle$ corresponds to the average over all configurations at a given concentration. The index $\perp$ shows that the MAE is calculated with respect to the magnetization along the surface normal z and the in-plane x or y direction. Lower panel: anisotropy of the averaged orbital magnetic moment for a 2×2, a pentamer, and a 3×3 cluster. $\langle\Delta L_{xz}\rangle=\langle L_x-L_z\rangle$, where $\langle\ \rangle$ refers to the average over all configurations.

the following we investigate the angular dependence—specified by the azimuthal angle φ—of the MAE for selected clusters, in order to illustrate the complex behavior of the in-plane anisotropy.

Figure 10 shows the dependence of the total MAE on the azimuth angle for the simple case of one Fe atom in a 3×3 Co cluster. Within this cluster the Fe atom can occupy three inequivalent sites—corner, edge, and center—and the direction of the easy axis, as well as the MAE strongly depends on the position of the Fe atom. For the cluster with the higher symmetry with respect to the x and y axes (Fe atom at center), the value of the anisotropy is very close to zero and its angular variation is only due to the cluster symmetry, which has a periodicity of 90° (inset of Fig. 10). If the Fe atom is located at the center of an edge the anisotropy energy is 2 orders of magnitude higher. In case the Fe atom sits on an edge parallel to the x axis, the easy magnetization axis is also along the x direction and the hard axis is perpendicular to it along the y direction. The periodicity of the angular variation of the MAE in this case is 180°, and the energy needed to switch the magnetization between two easy axes is identical to the amplitude. If the Fe atom is positioned at a
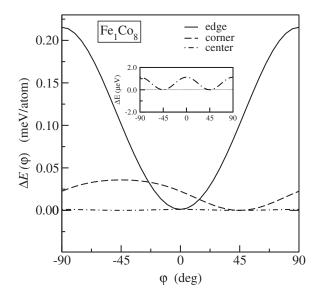
FIG. 10. Dependence of the anisotropy energy, $\Delta E(\varphi)=E(\varphi)-E(\varphi_0)$, with respect to different directions of the magnetization, specified by the azimuth angle φ. The three curves stand for the different configurations (cf. Fig. 12): No. 1, corner Fe atom (dashed line); No. 2, central Fe atom (dash-dotted line); No. 3, edge Fe atom (solid line).

FIG. 11. The anisotropy constants $K(\mathcal{C})$ for eight different configurations of Fe_2Co_7 cluster. The specified angles φ_0 refer to the direction of the easy axis of magnetization with respect to the cluster configurations. For each case, the corresponding configuration number (cf. Fig. 12) is indicated next to the symbols.

corner, then the easy axis is along $\varphi=45°$. Consequently the angular dependence of the MAE can be approximated by $\Delta E(\varphi)=K(\mathcal{C})\sin^2(\varphi-\varphi_0)$, where φ_0 is the direction of the easy magnetization axis, depending on the configuration symmetry, and $K(\mathcal{C})$ is an anisotropy constant, which is very sensitive to the specific cluster configuration $\mathcal{C}$.

As an additional illustration, Fig. 11 shows the values of the anisotropy constants $K(\mathcal{C})$ and the angles φ_0 of the easy axis for Fe_2Co_7. This cluster is distinguished from the previously discussed one by the appearance of two additional angles at $\varphi_0\approx23°$ and $\varphi_0\approx63°$ corresponding to the axes connecting the two Fe atoms of the cluster. The number at the left of each symbol refers to the corresponding cluster configurations as given in Fig. 12.

These simple cases illustrate the general features of more complicated ones, namely, that the direction of the easy axis is determined from the symmetry of the cluster configuration, and that the size of the anisotropy energy depends on the specific distribution of atoms. Clearly this means that by averaging over a large collection of clusters, where the exact individual configurations are not known, it is neither possible to predict the anisotropy energy, nor the direction of the easy axis of a single nanocluster.

IV. CONCLUSION

In this work we have determined the magnetic moments and the magnetic anisotropy of three different types of composite FeCo nanoclusters on a Cu(100) substrate by means of *ab initio* calculations. The study has concentrated on the effect of composition on the cluster properties, neglecting structural relaxation effects. While the atomic potentials are approximated as being spherically symmetric, higher mo-
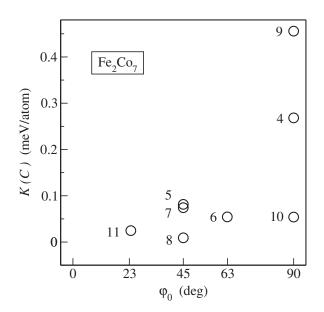
ments of the charge density have been taken into account. Clusters of three different geometries have been considered—2×2, crosslike pentamer, and 3×3—and the positions of the Fe and Co atoms have been varied according to all possible arrangements for given concentrations.

As in clusters of a pure material, the size of the spin magnetic moments depends on the position in the cluster for both, Fe and Co atoms, and consequently on the number of coordinated atoms as has been noticed previously by Mavropoulos *et al.*[34] In addition, depending on the atoms' position and on the geometry of the cluster, the spin moments show either no, or a high sensitivity to changes in the local environment, i.e., with respect to changes of the number or the position of the foreign atomic species.

Orbital moments are strongly influenced by the position of an atom. As has been found in many previous calculations[22,31,35–44] low coordinated atoms exhibit a significant increase of their orbital moments. In the present study it could be shown that they also depend on the specific cluster configurations and on the concentration of the atomic spe-
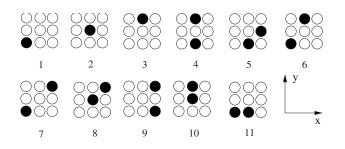

FIG. 12. Inequivalent configurations of 3×3 clusters containing one or two atoms, respectively, of a foreign species. The filled (empty) circles represent Fe (Co) atoms and vice versa.

cies. Moreover, low coordinated Co atoms, which have the largest moments within the surface plane, also exhibit a strong in-plane anisotropy of their orbital moments. Perimeter Fe atoms, in contrast, have strongly enhanced orbital moments along the z direction, perpendicular to the substrate surface.

By averaging over all possible cluster configurations, the total magnetic moments show a variation with respect to the concentration of Co atoms, which is very close to that found in monolayers of Fe_xCo_{1-x} as obtained from CPA calculations.

When evaluating the magnetic anisotropy energy it appears that the orientation of the easy axis depends on the cluster symmetry, originating from the distribution of the two different magnetic atoms. Then again, the size of the anisotropy energy is highly sensitive to the specific arrangements of atoms. Clusters which have a preferred in-plane magnetization direction are found to have an unusually large angle-dependent anisotropy energy. In these cases the direction of the easy axis will not necessarily be along the crystal axes,

but is determined by the specific distributions of Fe and Co atoms.

By plotting the MAE, averaged over all configurations, as a function of concentration of one atomic species, it is found that the easy magnetization direction of a collection of clusters can be tuned in a similar manner, as in thin films of the same materials,[45] by varying the concentration of the constituents.

[1] S. Rusponi, T. Cren, N. Weiss, M. Epple, P. Buluschek, L. Claude, and H. Brune, Nat. Mater. **2**, 546 (2003).

[2] K. von Bergmann, M. Bode, and R. Wiesendanger, Phys. Rev. B **70**, 174455 (2004).

[3] J. T. Lau, A. Fohlisch, R. Nietubyc, M. Reif, and W. Wurth, Phys. Rev. Lett. **89**, 057201 (2002).

[4] P. Gambardella, S. Rusponi, M. Veronese, S. S. Dhesi, C. Grazioli, A. Dallmeyer, I. Cabria, R. Zeller, P. H. Dederichs, K. Kern, C. Carbone, and H. Brune, Science **300**, 1130 (2003).

[5] A. Kubetzka, O. Pietzsch, M. Bode, and R. Wiesendanger, Phys. Rev. B **63**, 140407(R) (2001).

[6] D. Repetto, J. Honolka, S. Rusponi, H. Brune, A. Enders, and K. Kern, Appl. Phys. A: Mater. Sci. Process. **82**, 109 (2006).

[7] P. Bruno, Phys. Rev. B **39**, 865 (1989).

[8] P. Carra, B. T. Thole, M. Altarelli, and X. Wang, Phys. Rev. Lett. **70**, 694 (1993); B. T. Thole, P. Carra, F. Sette, and G. van der Laan, *ibid.* **68**, 1943 (1992).

[9] J. Kliewer, R. Berndt, and S. Crampin, Phys. Rev. Lett. **85**, 4936 (2000).

[10] M. Getzlaff, A. Kleibert, R. Methling, J. Bansmann, and K. H. Meiwes-Broer, Surf. Sci. **566**, 332 (2004).

[11] H. J. Richter, A. Y. Dobin, O. Heinonen, K. Z. Gao, R. J. M. v. d. Veerdonk, R. T. Lynch, J. Xue, D. Weller, P. Asselin, M. F. Erden, and R. M. Brockie, IEEE Trans. Magn. **42**, 2255 (2006).

[12] H. Brune, e-J. Surf. Sci. Nanotechnol. **4**, 478 (2006).

[13] N. Weiss, T. Cren, M. Epple, S. Rusponi, G. Baudot, S. Rohart, A. Tejeda, V. Repain, S. Rousset, P. Ohresser, F. Scheurer, P. Bencok, and H. Brune, Phys. Rev. Lett. **95**, 157204 (2005).

[14] G. A. Held, G. Grinstein, H. Doyle, S. Sun, and C. B. Murray, Phys. Rev. B **64**, 012408 (2001).

[15] H. Coufal, L. Dhar, and C. D. Mee, MRS Bull. **31**, 374 (2006); I. R. McFadyen, E. E. Fullerton, and M. J. Carey, *ibid.* **31**, 379 (2006); H. J. Richter and S. D. Harkness IV, *ibid.* **31**, 385 (2006).

[16] K. Mitsuzuka, N. Kikuchi, T. Shimatsu, O Kitakami, H. Aoi, H. Muraoka, and J. C. Lodder, IEEE Trans. Magn. **43**, 3883 (2006).

[17] H. J. Richter and A. Y. Dobin, J. Magn. Magn. Mater. **287**, 41 (2005).

[18] S. Sun and C. B. Murray, J. Appl. Phys. **85**, 4325 (1999).

[19] C. E. D. Smith, S. Khizroev, D. Weller, and D. Litvinov, IEEE Trans. Magn. **42**, 2411 (2006).

[20] D. Weller and A. Moser, IEEE Trans. Magn. **35**, 4423 (1999).

[21] C. P. Bean and J. D. Livingston, J. Appl. Phys. **30**, 120S (1959).

[22] B. Lazarovits, L. Szunyogh, and P. Weinberger, Phys. Rev. B **65**, 104441 (2003).

[23] D. M. Ceperley and B. J. Alder, Phys. Rev. Lett. **45**, 566 (1980); J. P. Perdew and A. Zunger, Phys. Rev. B **23**, 5048 (1981).

[24] S. Pick, V. S. Stepanyuk, A. N. Baranov, W. Hergert, and P. Bruno, Phys. Rev. B **68**, 104410 (2003).

[25] O. V. Lysenko, V. S. Stepanyuk, W. Hergert, and J. Kirschner, Phys. Rev. Lett. **89**, 126102 (2002).

[26] A. B. Shick, D. L. Novikov, and A. J. Freeman, J. Appl. Phys. **83**, 7258 (1998); A. B. Shick, D. L. Novikov, and A. J. Freeman, Phys. Rev. B **56**, R14259 (1997).

[27] R. Guirado-Lopez, M. C. Desjonqueres, and D. Spanjaard, Phys. Rev. B **62**, 13188 (2000).

[28] L. Szunyogh, B. Újfalussy, P. Weinberger, and J. Kollár, Phys. Rev. B **49**, 2721 (1994).

[29] H. J. F. Jansen, Phys. Rev. B **59**, 4699 (1999).

[30] G. M. Pastor, J. Dorantes-Davila, S. Pick, and H. Dreysse, Phys. Rev. Lett. **75**, 326 (1995).

[31] I. Cabria, B. Nonas, R. Zeller, and P. H. Dederichs, Phys. Rev. B **65**, 054414 (2002).

[32] P. Gambardella, S. Rusponi, T. Cren, N. Weiss, and H. Brune, C. R. Phys. **6**, 75 (2005).

[33] J. Dorantes-Davila, H. Dreysse, and G. M. Pastor, Phys. Rev. Lett. **91**, 197206 (2003).

[34] P. Mavropoulos, S. Lounis, R. Zeller, and S. Blügel, Appl. Phys. A: Mater. Sci. Process. **82**, 103 (2006).

[35] B. Lazarovits, L. Szunyogh, P. Weinberger, and B. Ujfalussy, Phys. Rev. B **68**, 024433 (2003); *ibid.* **67**, 024415 (2003); **73**, 045430 (2006).

[36] V. S. Stepanyuk, D. I. Bazhanov, A. N. Baranov, W. Hergert, P. H. Dederichs, and J. Kirschner, Phys. Rev. B **62**, 15398 (2000); V. S. Stepanyuk, W. Hergert, P. Rennert, K. Wildberger, R. Zeller, and P. H. Dederichs, *ibid.* **59**, 1681 (1999); **165**, 272 (1997).

[37] S. Pick, V. S. Stepanyuk, A. L. Klavsyuk, L. Niebergall, W. Hergert, J. Kirschner, and P. Bruno, Phys. Rev. B **70**, 224419 (2004).

[38] J. Dorantes-Davila and G. M. Pastor, Phys. Rev. Lett. **81**, 208 (1998).

[39] B. V. Reddy, S. N. Khanna, and B. I. Dunlap, Phys. Rev. Lett. **70**, 3323 (1993).

[40] B. Nonas, I. Cabria, R. Zeller, P. H. Dederichs, T. Huhne, and H. Ebert, Phys. Rev. Lett. **86**, 2146 (2001).

[41] K. Wildberger, V. S. Stepanyuk, P. Lang, R. Zeller, and P. H. Dederichs, Phys. Rev. Lett. **75**, 509 (1995).

[42] J. Minar, S. Bornemann, O. Sipr, S. Polesya, and H. Ebert, Appl. Phys. A: Mater. Sci. Process. **82**, 139 (2006).

[43] S. Bornemann, J. Minar, S. Polesya, S. Mankovsky, H. Ebert, and O. Sipr, Phase Transitions **78**, 701 (2005).

[44] Y. Xie and J. A. Blackman, Phys. Rev. B **66**, 155417 (2002).

[45] J. Zabloudil, L. Szunyogh, U. Pustogowa, C. Uiberacker, and P. Weinberger, Phys. Rev. B **58**, 6316 (1998).